OXIDATION OF OXALIC ACID IN AQUEOUS SUSPENSIONS OF SEMICONDUCTORS ILLUMINATED WITH UV OR VISIBLE LIGHT

JEAN-MARIE HERRMANN, MARIE-NOËLLE MOZZANEGA and PIERRE PICHAT
Institut de Recherches sur la Catalyse, Centre National de la Recherche Scientifique, 2 avenue Albert Einstein, 69626 Villeurbanne Cédex (France)

(Received December 9, 1982; in revised form January 31, 1983)

Summary

The behaviours of various semiconductor powders (TiO_2, Fe_2O_3, ZnO, ZrO_2, Sb_2O_4, CeO_2 and WO_3) dispersed in oxalic acid solutions were examined either in the dark or under illumination at wavelengths shorter or longer than 400 nm in the presence of oxygen. All the specimens except Sb_2O_4 and WO_3 were degraded in the dark, ZnO being the most unstable. UV illumination increased the oxidation of oxalic acid in the presence of TiO_2, ZrO_2 and CeO_2, and the quantum yields were determined. Visible light enhanced the conversion in the presence of TiO_2, Fe_2O_3 and WO_3. Despite its weak absorption, TiO_2 was the most reactive, and the two Fe_2O_3 samples exhibited markedly different activities. Doping of TiO_2 with Cr^{3+} ions (0.86 at.%) substantially decreased its activity in both spectral regions, probably because of increased electron–hole recombination. It is concluded from these results that the surface properties and the presence of recombination centres, which depend on the preparation method, are very important factors in determining the activity of a given oxide. The results of a more detailed study of the effects of oxygen, oxalic acid concentration, pH and temperature performed using the TiO_2 sample provided evidence for the photocatalytic character of the oxidation induced by UV light, and a mechanism involving an attack on the C—C bond of adsorbed $HC_2O_4^-$ ions by atomic oxygen species activated by photoproduced holes is tentatively suggested.

1. Introduction

The oxidizing properties of various semiconductor powders illuminated in either the near UV or the visible region were determined using oxalic acid. This compound was chosen because its reactivity allowed the stability of the solids employed to be assessed and also because it is a water pollutant resulting from some industrial treatment processes (textile industry, metallurgy etc.). Moreover, as indicated by the potential of the redox couple

0047-2670/83/$3.00

$H_2C_2O_4(aq)-CO_2(g)$ (−0.49 V), it is easy to oxidize and therefore even weakly oxidizing semiconductors should transform it.

Ions of simple carboxylic acids, such as formic, acetic or oxalic acid, have been used as scavengers of holes photoproduced from anodes formed by single crystals of TiO_2 [1, 2] or ZnO [3 - 5], thus causing the so-called current doubling effect. The oxidation of oxalate ions has been selected to test the photoresponse of metal phthalocyanine evaporated film electrodes [6]. The photocatalytic oxidation of formic acid over TiO_2 dispersed in an aqueous solution has been studied as a function of the UV light intensity and of the acid and dissolved oxygen concentrations [7]. Formic and oxalic acids have been used to scavenge $OH^{\cdot}$ radicals in the photosynthesis of H_2O_2 over ZnO and the evolution of CO_2 was observed [8]. The photocatalytic decarboxylation of acetic acid and of a series of other organic acids over TiO_2 and $Pt-TiO_2$ in the absence of oxygen is well documented [9].

In the present work we studied the stability of various semiconductors in the dark and the effect of illumination at wavelengths shorter or longer than 400 nm on their reactivity. The most active sample (TiO_2) was used for an investigation of the effects of the reactant concentration, oxygen, pH and temperature under UV illumination. A photocatalytic mechanism is tentatively proposed on the basis of our previous results concerning the photocatalytic activation of oxygen [10 - 15] and its reactivity with organic [11, 15 - 17] and inorganic [18, 19] compounds.

2. Experimental details

The heterogeneous photocatalytic oxidation of oxalic acid was studied using a cylindrical static slurry photoreactor with an optical quartz base. The temperature (270 - 352 K) was controlled by means of a thermostatted jacket. The catalyst suspension (50 mg in 20 cm^3) was stirred by a rotating T-shaped capillary glass tube through which oxygen flowed at a constant rate of 10 cm^3 min^{-1}. Under these conditions optimum oxygen interaction with the solid surface through the aqueous phase and complete light absorption by the solid particles were achieved. The illumination was provided by a mercury lamp (Philips HPK 125 W) in the UV region and by a xenon lamp (Hanovia 150 W) in the visible region. In both cases the IR fraction of the beam was removed by a water circulating cuvette which was terminated by filters which limited the transmitted wavelengths to the ranges 300 - 400 nm (Corning 7-60 filter) and 400 - 660 nm (combined Corning 0-51 and 4-97 filters).

The conversion rate was calculated by determining the quantity of unreacted oxalic acid using conventional permanganate titration. The formation of gaseous CO_2 was detected qualitatively by bubbling the excess oxygen into a solution of barium nitrate.

3. Results

3.1. Reaction in the absence of suspended solid

Stirred and oxygenated oxalic acid solutions were stable for at least 6 h under visible light at the radiant intensity employed. Under UV illumination negligible photochemical conversion, which depended on the concentration, occurred (compare Tables 1 and 2).

TABLE 1

Photochemical conversion of oxalic acid under UV illumination

Initial concentration (M)	*Illumination time* (h)	*Conversion* $\tau = (C_0 - C)/C_0$ (%)	*Mean photochemical activity* (mol h^{-1})
5×10^{-2}	6	2	3.3×10^{-6}
5×10^{-3}	6	4	6.7×10^{-7}

C_0, initial concentration; C, concentration at time t.

TABLE 2

Conversion of oxalic acid ($C_0 = 5 \times 10^{-3}$ M) within a period of 30 min over various oxides under UV illumination and in the dark

Catalyst	*Origin*	*Specific area* ($m^2 g^{-1}$)	*Stability in oxalic acid*	*Overall conversion* (%)	*Conversion in the dark* (%)	*Mean photocatalytic activity* (μmol h^{-1})	*Mean quantum yield*
TiO_2	Degussa P-25	50	Rather stable	48	8	80	0.34
ZnO	Merck	3	Quite unstable	75	78	—	—
ZrO_2	[20]	37	Corrodes	51	18	66	0.28
CeO_2	[21]	27	Corrodes	29	16	26	0.11
Sb_2O_4	[22]	2.7	Inert	0	0	0	0
Cr^{3+}–TiO_2	[20]	60	Rather stable	8.5	8	1	0.004

3.2. Reaction in the presence of a solid in the dark

All the solids except Sb_2O_4 and WO_3 were active with respect to oxalic acid in the dark and under oxygen flow (Tables 2 and 3). Therefore the corresponding conversions were subtracted from those obtained in the presence of illumination to determine the effects of UV and visible light.

3.3. Effects of various parameters on the reaction induced by UV-illuminated TiO_2

TiO_2 was chosen because it had the highest photocatalytic activity (Table 2).

TABLE 3

Conversion of oxalic acid ($C_0 = 5 \times 10^{-3}$ M) over various oxides under visible illumination and in the dark

Catalyst	*Origin*	*Specific area* ($m^2 g^{-1}$)	*Reaction time* (min)	*Overall conversion* (%)	*Conversion in the dark* (%)	*Mean photocatalytic activity* (μmol h^{-1})
TiO_2	Degussa P-25	50	30	18.4	7.8	21
Cr^{3+}–TiO_2	[20]	60	30	7.9	7.8	0.24
Fe_2O_3 (1)	Merck	< 5	180	13.5	5.9	2.5
Fe_2O_3 (2)	Amorphous[a]	146	180	75.5	15.7	20
WO_3	[23]	15	180	28.7	0	9.6

[a] Hydrated solid obtained by precipitation at pH 8.

3.3.1. Effect of the concentration

A typical plot of the overall conversion τ in per cent as a function of time is shown in Fig. 1 ($\tau = (C_0 - C)/C_0$ where C_0 is the initial concentration

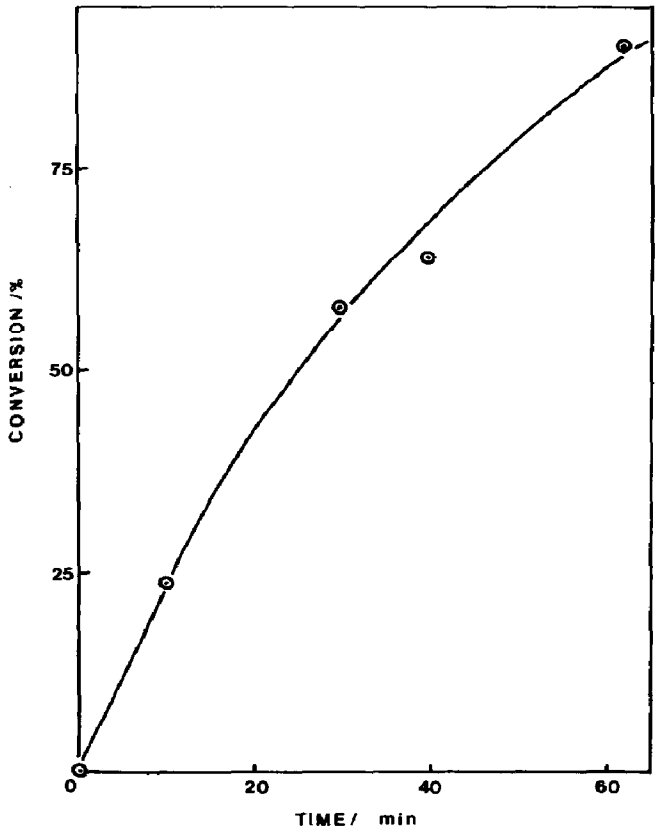

Fig. 1. Overall conversion of oxalic acid ($C_0 = 5 \times 10^{-3}$ M) over TiO_2 as a function of the UV illumination time.

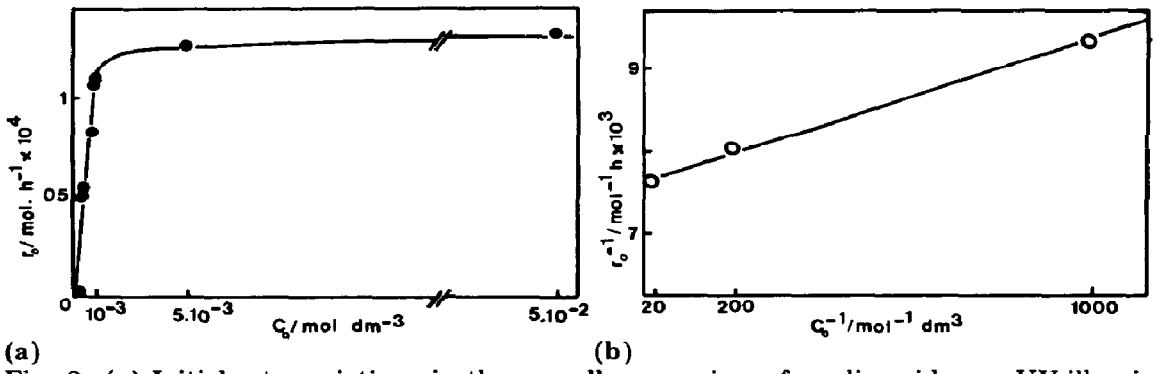

(a) (b)

Fig. 2. (a) Initial rate variations in the overall conversion of oxalic acid over UV-illuminated TiO_2 as a function of the initial concentration; (b) linear transform of the curve shown in (a).

and C is the concentration at time t). The reproducibility was within 4%. The curve of the plot is ascribed to the progressive consumption of oxalic acid ions in the static reactor. Therefore the initial reaction rate r_0 determined in the first 10 min was used in the investigation. r_0 varied as a function of C_0 according to a Langmuir-type isotherm (Fig. 2) so that it was almost independent of C_0 for $C_0 > 5 \times 10^{-3}$ M, which confirmed the apparent zero order found for the oxidation of formic acid [7], and decreased sharply for $C_0 < 10^{-3}$ M.

3.3.2. Effect of oxygen

The oxygen flow rate was about a factor of 200 greater than that required for the initial reaction rate.

In the absence of oxygen (the suspension was deaerated by several evacuations in a closed photoreactor) the rate of oxidation of oxalic acid decreased and the TiO_2 gradually became greyish blue. After UV illumination for 3 h the conversion of oxalic acid was equal to that obtained in the presence of oxygen after illumination for a period about a factor of 14 shorter.

3.3.3. Effect of the pH

Figure 3 shows that when the pH was varied from zero (addition of H_2SO_4) to 13 (addition of NaOH) the photocatalytic activity reached a maximum at pH 2.34 (pure oxalic acid) where 93% of the oxalic acid ions are present as $HC_2O_4^-$ and was zero at pH 13 where most of the ions are present as $C_2O_4^{2-}$. It should be noted that the pH variations (1.5 - 3.0) induced by diluting pure oxalic acid (Fig. 2) did not modify the major ionization state of oxalic acid ($HC_2O_4^-$) whose coverage remained almost unchanged as calculated using the adsorption constant given in Section 4.1.

3.3.4. Effect of temperature

The variations in the conversion are presented in the Arrhenius plot of Fig. 4. The apparent activation energy is 13 kJ mol^{-1} which is in the

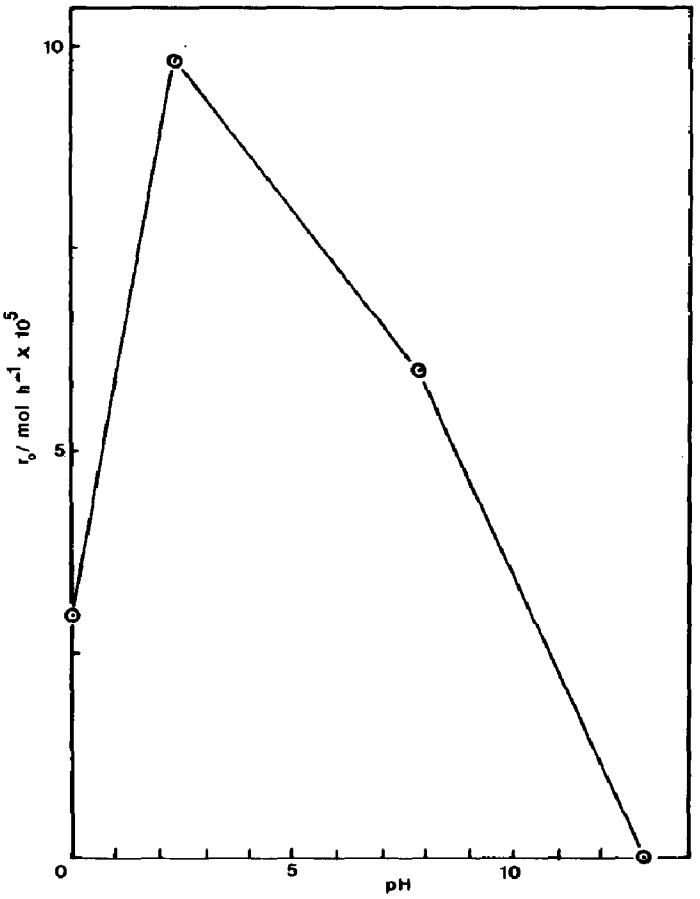

Fig. 3. Initial rate of the overall conversion of oxalic acid ($C_0 = 5 \times 10^{-3}$ M) over UV-illuminated TiO_2 as a function of the pH.

same range as that obtained for the oxidation of formic acid under similar conditions [7].

3.4. Effect of the nature of the solid

3.4.1. UV illumination

The quantum yields were defined as the ratio ϕ of the number of molecules converted per second to the number of photons, which can be absorbed by the oxide, entering the cross-sectional area S of the photo-reactor per second:

$$\phi = \frac{C_0 V(\mathrm{d}\tau/\mathrm{d}t)N}{FPS}$$

where V is the volume of the solution, N is Avogadro's number, F is the flux of absorbable photons per unit of power, P is the incident light power (3.1 mW cm^{-2}) and S is the cross-sectional area of the reactor (11.3 cm^2).

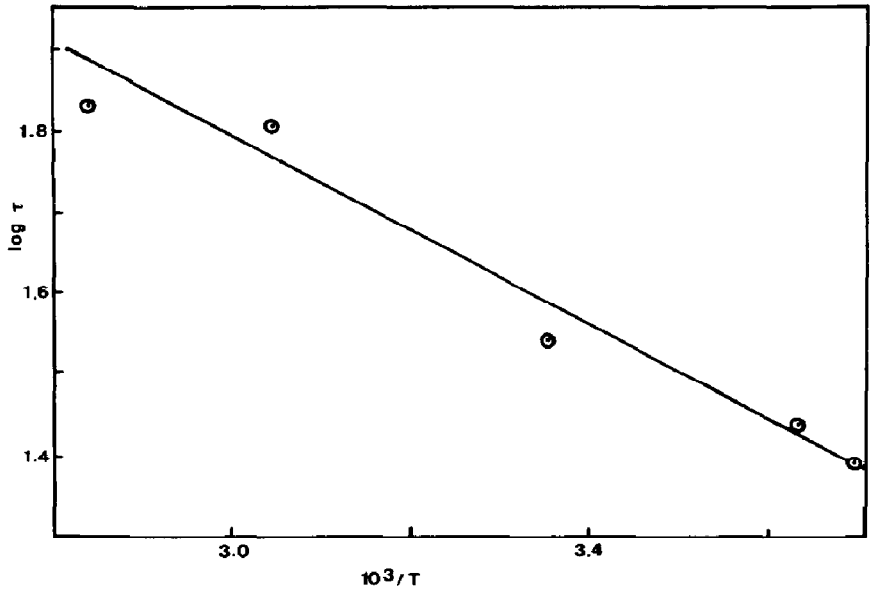

Fig. 4. Arrhenius plot of the overall conversion of oxalic acid ($C_0 = 5 \times 10^{-3}$ M) over TiO_2 (UV illumination for 20 min).

F was calculated from the wavelength dependence of the absorption coefficient of each oxide as determined from the reflectance spectra [17, 19]. The quantum yields are listed in Table 2.

3.4.2. Visible illumination

The mean photocatalytic activities of the most active solids are presented in Table 3. Other solids, such as CdS, Sb_2S_3 (commercial samples) and MoS_2 (various samples prepared in the laboratory for hydrodesulphurization reactions), yielded only traces of products.

4. Discussion

It is necessary to establish over which solids the oxidative degradation of oxalic acid is really photocatalytic, which requires that (i) the activation by light is due to the solid and (ii) at least one step of the reaction occurs in the adsorbed phase.

The photochemical oxidation was either absent (visible light) or almost negligible (UV light) under oxygen flow. When a solid is present its corrosion resulting from the acidic and redox properties of the oxalic acid solution should be distinguished from the true photocatalytic process.

4.1. Photocatalytic character and mechanism of oxidation over UV-illuminated TiO_2

The photocatalytic character of the reaction is shown (i) by the Langmuir character of the isotherm in Fig. 2 which implies that the reaction

takes place in the adsorbed phase and (ii) by the observation that a greater number of oxalic acid molecules are oxidized than that which could have been obtained from the photoactivatable surface species initially present at the surface of TiO_2 (a maximum of five such species per nanometre squared was assumed).

If the reaction of adsorbed oxalic acid ions with adsorbed oxygen species is involved the initial reaction rate can be written

$$r_0 = kf[O_2]\theta_0$$

where k is the rate constant of the reaction, $f[O_2]$ is a function of the surface concentration of oxygen species and θ_0 is the initial surface coverage by oxalic acid. Since the flow rate and the solubility of oxygen in water are constant, $f[O_2]$ can be considered as a constant and included in the apparent rate constant k'. θ_0 can be replaced by $KC_0/(1 + KC_0)$ according to the Langmuir-type isotherm (K is the adsorption constant of oxalic acid) so that the expression

$$r_0 = k' \frac{KC_0}{1 + KC_0}$$

is obtained in agreement with the linear transform of Fig. 2(b) whose slope $(k'K)^{-1}$ and intercept k'^{-1} yield

$$k' = 1.3 \times 10^{-4} \text{ mol h}^{-1}$$

$$K = 4.4 \times 10^{3} \text{ dm}^3 \text{ mol}^{-1}$$

Only the points for high concentrations were included in Fig. 2(b) because of the low accuracy of the results for small concentrations. According to the value of K, the coverage θ_0 at $C_0 = 5 \times 10^{-3}$ M is 95.6% of its maximum. The linear variation in r_0^{-1} with C_0^{-1} implies a non-dissociative adsorption of $HC_2O_4^-$ which is the major ionized form of oxalic acid.

The experiments performed in the absence of oxygen indicate that this gas is essential. Furthermore, the observation that TiO_2 became greyish blue in colour suggests that the reaction involves surface oxygen species and increases the non-stoichiometry of O^{2-} anions from TiO_2. For example after 3 h of UV illumination, 6.8 molecules of oxalic acid were oxidized per nanometre squared of TiO_2. Consequently, if it is assumed that the most probable crystallographic plane present at the surface of TiO_2 is the (001) plane [24], about 0.5 oxalic acid molecules are converted per axial oxygen atom. Dissolved oxygen (3.1×10^{-2} cm^3 O_2 (cm^3 H_2O)$^{-1}$) does not behave as an electrolyte and does not compete with the other ions present in the solution with respect to adsorption. Even water does not compete with gaseous oxygen for electron capture as shown by previous photoconductivity measurements in the gas phase. Consequently, we assume that the ionosorbed oxygen species on the surface of the TiO_2 particles suspended in water are the same as those present in the gas phase. These species were identified by photoconductivity measurements as O_2^- and O^- [14]. *In situ* determinations

[11] have shown that the activation of oxygen occurs via the neutralization of ionosorbed O^- species by photoproduced holes:

$$(TiO_2) + h\nu \longrightarrow e^- + p^+$$

$$O^-_{ads} + p^+ \longrightarrow O^*_{ads}$$

($h\nu \geqslant E_g$ where E_g is the energy band gap). Consequently a mechanism involving the reaction of the photoactivated species O_{ads}^* with adsorbed $HC_2O_4^-$ ions is tentatively suggested since these ions are the most reactive form of oxalic acid according to the pH dependence of the photocatalytic activity (Fig. 3) and in agreement with ref. 25. Three different points of attack on the ion can be envisaged:

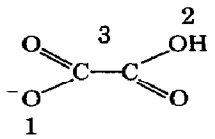

If the oxidation proceeded through the ionized extremity (point 1), a higher yield would be obtained for the doubly ionized ions $C_2O_4^{2-}$ present at alkaline pH. This is not the case as can be seen in Fig. 3. Similarly, the oxidation via the OH group of the molecule (point 2) can be rejected since it would give a maximum activity at acidic pH where oxalic acid is essentially present as $H_2C_2O_4$ molecules. This suggests that degradation occurs by an attack on the C—C bond (point 3) with the production of a possible epoxide intermediate leading to the formation of a CO_2 molecule plus an unstable bicarbonate ion [26] which in turn generates a second CO_2 molecule:

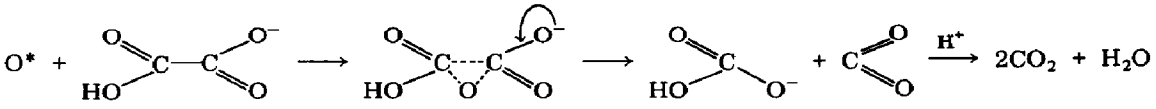

As the photocatalytic activation process is not temperature dependent, the low activation energy (13 kJ mol^{-1}) can be related to a step following the activation of oxygen, probably the CO_2 desorption.

4.2. Oxidation over UV-illuminated ZnO, ZrO_2, CeO_2 and Sb_2O_4

ZnO corroded at such a rate that no illumination effect could be observed. This marked corrosion is in agreement with the well-known basicity of ZnO [27]. The relative order of the quantum yields for the photocatalytic activities of the other oxides (Table 2) is identical with that found for the gas phase oxidation of propene [17], with the exception of Sb_2O_4 which is inactive. This probably arises from an identical activation process for both reactions in the gaseous and the liquid phases. The existence of O^- species at the surface of ZrO_2 and CeO_2 has been inferred from mea-

surements of the photoconductivity as a function of the oxygen pressure [14]. However, the relative ratios of the quantum yields for the various oxides differed from those found in propene oxidation.

4.3. Illumination in visible light

Three major facts can be noted from the results of Table 3.

(i) Surprisingly, the TiO_2 sample was the most active (together with Fe_2O_3 (2)) although its photocatalytic activity per radiant flux was about 260 times smaller in the visible region than in the UV region. This photosensitivity of TiO_2 in the visible region can be ascribed to an absorption tail for $\lambda > 400$ nm which is probably due to structural defects related to its highly divided state as previously found for the photoresponse of single-crystal and polycrystalline ZnO samples [28]: however, this poor photosensitivity is partially compensated by chemisorptive and catalytic properties which enable TiO_2 to surpass other solids whose band gap energies fit the visible spectrum better.

(ii) The doping of TiO_2 with Cr^{3+} ions markedly reduced the conversion despite the increased absorbance in the visible region. Presumably, these cations act as recombination centres [29].

(iii) The two samples of Fe_2O_3 prepared by different methods had very distinct photocatalytic activities.

All these observations emphasize the fact that the photocatalytic activity depends not only on the chemical nature of the sample but also on its surface and textural properties, *i.e.* its catalytic sites and recombination centres. Therefore any classification of the photocatalytic properties of semiconductors should be considered as relative and only valid for the samples used.

Acknowledgments

The authors thank Mrs. M. Besson-Andres and Dr. P. Vergnon for the gift of the Fe_2O_3 and Cr^{3+}–TiO_2 samples respectively.

References

1 E. C. Dutoit, F. Cardon and W. P. Gomes, *Ber. Bunsenges. Phys. Chem.*, *80* (1976) 1285.
2 Y. Maeda, A. Fujishima and K. Honda, *J. Electrochem. Soc.*, *128* (1981) 1731.
3 W. P. Gomes, T. Freund and S. R. Morrisson, *J. Electrochem. Soc.*, *115* (1968) 818.
4 S. R. Morrisson and T. Freund, *J. Chem. Phys.*, *47* (1967) 1543.
5 K. Micka and H. Gerischer, *J. Electroanal. Chem.*, *38* (1972) 397.
6 S. Meshitsuka and K. Tamaru, *J. Chem. Soc., Faraday Trans. I*, *73* (1977) 236.
7 M. Bideau, B. Claudel and M. Otterbein, *J. Photochem.*, *14* (1980) 291.
8 J. R. Harbour and M. L. Hair, *J. Phys. Chem.*, *83* (1979) 652.

9 B. Kraeutler and A. J. Bard, *J. Am. Chem. Soc., 99* (1977) 7729; *100* (1978) 5985; *Nouv. J. Chim., 3* (1979) 31.
I. Izumi, F.-R. F. Fan and A. J. Bard, *J. Phys. Chem., 85* (1981) 218.
10 J.-M. Herrmann, J. Disdier and P. Pichat, in R. Dobrozemsky, F. Rüdenauer, F. P. Viehböck and A. Breth (eds.), *Proc. 7th Int. Vacuum Congr. and 3rd Int. Conf. on Solid Surfaces, Vienna, September 12 - 16, 1977*, Vol. 2, Berger Söhne, Horn, 1977, p. 951.
11 J.-M. Herrmann, J. Disdier, M.-N. Mozzanega and P. Pichat, *J. Catal., 60* (1979) 369.
12 H. Courbon, M. Formenti and P. Pichat, *J. Phys. Chem., 81* (1977) 550.
13 H. Courbon and P. Pichat, *C.R. Acad. Sci., Sér. C, 285* (1977) 171.
14 J.-M. Herrmann, J. Disdier and P. Pichat, *J. Chem. Soc., Faraday Trans. I, 77* (1981) 2815.
15 P. Pichat, J.-M. Herrmann, H. Courbon, J. Disdier and M.-N. Mozzanega, *Can. J. Chem. Eng., 60* (1982) 27.
16 M.-N. Mozzanega, J.-M. Herrmann and P. Pichat, *Tetrahedron Lett., 34* (1977) 2965.
17 P. Pichat, J.-M. Herrmann, J. Disdier and M.-N. Mozzanega, *J. Phys. Chem., 83* (1979) 3122.
18 H. Mozzanega, J.-M. Herrmann and P. Pichat, *J. Phys. Chem., 83* (1979) 2251.
19 J.-M. Herrmann and P. Pichat, *J. Chem. Soc., Faraday Trans. I, 76* (1980) 1138.
20 F. Juillet, F. Lecomte, H. Mozzanega, S. J. Teichner, A. Thevenet and P. Vergnon, *Faraday Symp. Chem. Soc., 7* (1973) 57.
21 M. Guénin, *Ann. Chim. (Paris), 8* (1973) 147.
22 J.-M. Herrmann, J.-L. Portefaix, M. Forissier, F. Figueras and P. Pichat, *J. Chem. Soc., Faraday Trans. I, 75* (1979) 1346.
23 J. E. Germain and R. Laugier, *Bull. Soc. Chim. Fr.*, (1972) 541.
24 M. Primet, P. Pichat and M.-V. Mathieu, *J. Phys. Chem., 75* (1971) 1216.
25 Z. D. Draganic, M. M. Kosanic and M.-T. Nenadovic, *J. Phys. Chem., 71* (1967) 2390.
26 M. Primet, P. Pichat and M.-V. Mathieu, *J. Phys. Chem., 75* (1971) 1221.
27 T. Yamanaka and K. Tanabe, *J. Phys. Chem., 79* (1975) 2409.
28 Y. Shapira, S. M. Cox and D. Lichtman, *Surf. Sci., 54* (1976) 43.
29 G. Campet, J. Verniolle, J.-P. Doumerc and J. Claverie, *Mater. Res. Bull., 15* (1980) 1135.